

Strength estimation for FRP wrapped reinforced concrete columns

Hsiao-Lin Cheng[†]

*Department of Civil Engineering, Chung Cheng Institute of Technology, CCIT,
Yuanshulin, Tähsü, Taoyuan, 33508, Taiwan*

Elisa D. Sotelino[‡]

School of Civil Engineering, Purdue University, W. Lafayette, IN 47907, U.S.A.

Wai-Fah Chen^{††}

College of Engineering, University of Hawaii, Honolulu, HI 96822, U.S.A.

Abstract. Fiber-Reinforced Plastics (FRP) have received significant attention for use in civil infrastructure due to their unique properties, such as the high strength-to-weight ratio and stiffness-to-weight ratio, corrosion and fatigue resistance, and tailorability. It is well known that FRP wraps increase the load-carrying capacity and the ductility of reinforced concrete columns. A number of researchers have explored their use for seismic components. The application of concern in the present research is on the use of FRP for corrosion protection of reinforced concrete columns, which is very important in cold-weather and coastal regions. More specifically, this work is intended to give practicing engineers with a more practical procedure for estimating the strength of a deficient column rehabilitated using FRP wrapped columns than those currently available. To achieve this goal, a stress-strain model for FRP wrapped concrete is proposed, which is subsequently used in the development of the moment-curvature relations for FRP wrapped reinforced concrete column sections. A comparison of the proposed stress-strain model to the test results shows good agreement. It has also been found that based on the moment-curvature relations, the balanced moment is no longer a critical moment in the interaction diagram. Besides, the enhancement in the loading capacity in terms of the interaction diagram due to the confinement provided by FRP wraps is also confirmed in this work.

Key words: Fiber-Reinforced Plastics (FRP); columns; concrete; strength; ductility; confinement.

1. Introduction

In many countries around the world, there is a tremendous need to repair and strengthen the existing infrastructure as a result of aging, seismic activity, environmental degradation, code change, construction or design defects, misuse, poor maintenance, change in use, etc. In the United States, for example, many of the nation's bridges and other civil engineering structures are deteriorating due to problems associated with

[†]Assistant Professor

[‡]Associate Professor of Structural Engineering

^{††}Professor and Dean

reinforced concrete. According to the report conducted by the Federal Highway Administration (FHWA), it has estimated that over 240,000 (about 40%) of the highway bridges are either functionally or structurally deficient, and that it would cost about \$300 billion just to maintain this status (Lan *et al.* 1998). Therefore, there is an urgent need to develop methods to prevent structures from further deteriorating, and to restore them to a level that is rationally accepted. For reinforced concrete columns, a number of retrofit techniques have been developed and tested. They include steel jacketing, active confinement by wire prestressing, concrete jacketing, and the use of composite-materials jackets (Priestley *et al.* 1996). Among them, composite-materials jackets have drawn the greatest attention from civil engineers due to their unique properties.

In general, this technique consists of using composite materials, such as carbon fibers, glass fibers, and Kevlar fibers, bonded together and to the column with resins. Composite materials or Fiber-Reinforced Plastics, called FRP herein, have received significant attention for use in civil infrastructure due to their unique properties, such as the high strength-to-weight ratio and stiffness-to-weight ratio, corrosion and fatigue resistance, and tailorability. In this technique, FRP sheets are wrapped around the column to form a protective jacket with the major fibers running in the hoop direction, to serve as external confinement of the column, and to form a hybrid system with the reinforced concrete column. It has been shown that this hybrid system with confinement provided by FRP increases both the compressive strength and ductility of the column (Fardis and Khalili 1981, 1982, Demers and Neale 1994, Saadatmanesh *et al.* 1994, 1996, Nanni and Bradford 1995, Karbhari and Howie 1995, 1997, Mirmiran and Shahawy 1997). Also it has been demonstrated that FRP jacketing can be as effective as conventional steel jacketing in improving the seismic response characteristics of substandard reinforced concrete columns (Seible *et al.* 1997). Besides, FRP is an excellent corrosion resistant material and, when wrapped onto the column, acts as an additional barrier against steel corrosion in addition to the barrier provided by concrete. It can, thus, enhance the durability of the columns as well (Teng *et al.* 2000). Right now, the use of FRP has become one of the fastest growing new areas in civil infrastructure, especially for column retrofits.

Although the civil engineering community, government organizations, and other industry have dedicated significant efforts to this field, some impediments still exist in the use of this technique. One of the major impediments is the lack of confidence on these hybrid systems, due to the lack of experience with them. Design procedures and guidelines would help improve the confidence of engineers in using such systems. However, at this time, much of the available criteria have been developed for FRP wraps used for seismic retrofit of structural components. The application of concern in the present research is on the use of FRP to repair deteriorated reinforced concrete columns, which occurs in cold-weather and coastal regions. More specifically, this work is intended to give practicing engineers with a procedure for quickly estimating the strength of a deficient column rehabilitated using FRP wrapped columns. More specifically, a stress-strain relation for these hybrid column systems is proposed. Based on this fundamental relation, the moment-curvature relationship is then developed analytically. It should be noted that this relationship is the basic tool in the analysis of an FRP wrapped beam-column problem.

The authors are currently investigating the behavior of the new hybrid system by means of a sensitivity study, based on the moment-curvature relations developed in the present work. A design equation or a simple interaction equation is being sought. The goal of the final product is to help engineers to take advantage of these systems in civil infrastructure with more confidence. Furthermore, a practical extension of the present research would be the development of design guidelines for deteriorated columns rehabilitated using FRP wraps. The use of this technology to this

type of application would provide an economical way of restoring the original strength of deficient columns.

2. Previous research

Even though the concept of confinement effects on concrete strength and ductility has been studied the development of a stress-strain relation for FRP wrapped concrete is relatively new. Several FRP jacketing systems have been developed and validated via laboratory or field experiments. They include prefabricated FRP tubes, prefabricated FRP shells, and FRP wraps, and are described next.

2.1. Prefabricated FRP tubes

Prefabricated FRP tubes, called FRP tubes, can be traced back to 1978 (Kurt 1978). In this work commercially available plastic pipes (PVC or ABS) filled with concrete were tested. It was found that plastic pipes are more effective in confining concrete than steel pipes. However, no significant increase in concrete strength was observed, since the plastic pipes used in his experiments were not strong or stiff enough.

Fardis and Khalili (1981, 1982) suggest that the ideal form of an FRP concrete system is one in which the concrete is encased in an FRP tube. The FRP tube system provides several advantages. It increases the strength and ductility of concrete because of confinement, it acts as a pour form to reduce the cost and increase the speed of the construction, and it serves as a protective jacket and external reinforcement for concrete improving its durability and watertightness. This system is more advantageous when it has a higher density of fibers in the circumferential direction. However, even though they proposed the concept of using an FRP tube as a pour form, their tests dealt only with glass FRP wrapped concrete.

A similar FRP tube system was proposed by Mirmiran and Shahawy (1997). In their work, the tube was a multi-layer composite shell that consisted of at least two plies: an inner ply of axial fibers, and an outer ply of hoop fibers. It possessed the same advantages as the FRP tube proposed by Fardis & Khalili. This FRP tube is most suitable in new construction, and can be used to reduce the labor costs in the field because the presence of bi-directional fibers in the FRP tube eliminates the need for conventional steel reinforcement in the column altogether. FRP tubes can also be considered as an extension of conventional steel tubes.

In the work by Seible *et al.* (1996), two design concepts that considered pre-manufactured filament wound carbon tubes as reinforcement for concrete columns were investigated. In the first design, large inelastic rotations at the base were allowed, while in the second design the FRP shell extended into the concrete footing. Both designs were compared to conventional reinforced concrete design by means of laboratory tests in which simulated seismic loads were used. They found that the response obtained for columns designed using the first concept was very close to that of conventional RC columns. For the second design, on the other hand, early failure due to high stress concentrations at the footing interface was observed.

2.2. Prefabricated FRP shells

Researchers at Penn State University developed a prefabricated FRP shell, referred to as FRP shell herein. In this system a FRP shell is manufactured in two halves, and then bonded in the field with

cement grout to fill the void between the shell and the column (Nanni and Bradford 1995). Tests showed that the glass-aramid shell system increases the strength and ductility of the concrete, but is not as effective as a fiber wrapping system because of the presence of joints, which tended to fail first.

Another similar FRP shell system was proposed by Xiao and Ma (1997). Their system used a series of prefabricated E-glass FRP shells with slits. When applied in a column, the shells were opened and clamped around the column in sequence with their slits staggered. Adhesive was then used to bond the shells to the column to form a jacket. The effectiveness of these FRP shells has been found to improve the seismic performance of circular reinforced columns having poor lap-spliced reinforcement details (Xiao *et al.* 1996, Xiao and Ma 1997).

2.3. FRP straps

Saadatmanesh *et al.* (1994) also introduced a system, called FRP straps, for column retrofit. Both E-glass fiber straps and carbon fiber straps made of resin-impregnated unidirectional fibers were used. They indicated significant increases in compressive strength and ductility of concrete as the strap spacing decreased. Saadatmanesh *et al.* (1996) again used unidirectional E-glass fiber straps to wrap concrete columns only in the potential plastic hinge region. They found similar results; i.e., a significant improvement in both strength and ductility was observed for columns externally wrapped with FRP straps in the potential plastic hinge region.

2.4. FRP wraps

The FRP wrap system is the simplest and the most widely used in column retrofit. It involves either the hand lay-up process or the filament winding process, which places the fibers and the resin in the field on the surface of an existing column. In the studies by Fardis and Khalili (1981, 1982), 46 axial compression tests were conducted on 2 different sizes of concrete cylinders wrapped with 4 different types of glass FRP (GFRP) sheets. In all tests, failure occurred by fracture of the FRP in the circumferential direction. They concluded that under short-term loads, concrete cylinders with GFRP have high strength and satisfactory ductility.

Demers and Neale (1994) investigated a total of 20 concrete specimens with circular or square shape, of which 14 were wrapped with unidirectional GFRP or carbon FRP (CFRP) sheets. Tests indicated the potentially beneficial effects of FRP wrapping, such as improving the strength and the ductility of concrete columns. In certain cases, it was observed that increases in strength of up to 70% are possible, and that the strain to failure can be of the order of 7 times that of an unconfined specimen.

A total of 27 cylinders and short concrete columns wrapped by unidirectional carbon FRP (CFRP) sheets at different wrapping configurations were investigated by Picher *et al.* (1996). They found that the confinement of concrete cylinders with CFRP sheets improves their compressive strength and ductility.

Karbhari and Howie (1995, 1997) investigated the effects of the fiber orientation and of the number of layers on the compressive strength of concrete cylinders. Unidirectional carbon FRP sheets were used in this case. Tests showed that the strength of the confined specimens increases with the increase of the number of layers in the hoop direction.

Priestley and Seible (1991) and Seible and Priestley (1993) conducted several large-scale tests on seismic retrofits with FRP wraps. 40% scale bridge piers wrapped with GFRP were tested under cyclic flexural loads. Their tests indicated significant improvement of seismic performance with increased ductility.

3. Scope

Due to the complexity of the hybrid system and the variety of applications of FRP on concrete columns, this paper is limited to the following:

- (1) Only short-term behavior of an FRP wrapped reinforced concrete column is considered. In other words, effects of creep and shrinkage are ignored.
- (2) The fiber directions in the FRP wraps are placed in the hoop of the concrete column. Because the enhancement in strength and ductility of the FRP wrapped reinforced concrete column is attributed to the confinement provided by FRP wraps, the confinement is most efficient when fibers are placed in the hoop direction.
- (3) Only FRP wrapped reinforced concrete columns with circular cross-sections are considered. It is well known that the confinement of FRP wraps greatly increases both the ductility and the strength of hybrid columns for circular sections. For rectangular cross-sections, however, the increase in ductility and strength is much smaller.

4. Stress-strain relations for FRP wrapped concrete

Four different FRP jackets have been discussed in the previous section. They include prefabricated FRP tubes, prefabricated FRP shells, FRP straps, and FRP wraps. Although the same concepts of FRP confinement and concrete expansion apply to all of them, there is one major difference amongst them that may lead to different degrees of confinement and in turn affect the capacity of the column. One of the major differences is the bond action between FRP jackets and the concrete core (Mirmiran and Shahawy 1997). For the application of FRP wraps, epoxy is applied on the column before FRP is wrapped around the column. In this case, the FRP jackets are biaxially loaded in both hoop and axial directions even though the column is subjected to uniaxial compression. On the other hand, the prefabricated tubes or shells usually have a smooth interior surface without chemical bond between the FRP and the concrete core. Mastrapa (1997) conducted tests to evaluate the bond effect on the confinement. Fiber-wrapped columns and concrete-filled tubes, considered as bonded and unbonded cases respectively, were used. It was concluded that the bond effect on FRP-confined concrete is not significant. Therefore, the bond action between the FRP jackets and the concrete core is ignored in this paper.

In the development of the stress-strain curve of concrete, there is no “exact” theory available. The only actual basis for comparison is the curve derived from experimental results (Saenz 1964). Besides, the stress-strain relation depends on several factors, such as properties of concrete and confining materials, and the interaction amongst these factors. Therefore, the best way to develop a suitable stress-strain model for FRP wrapped concrete is to use valuable test results from different studies.

A model has been developed to predict the stress-strain relation of FRP wrapped concrete. While other confined concrete models exist, such as those by Picher *et al.* (1996), Spolestra and Monti (1999), and Xiao and Wu (2000), the present model adopts the same form as that of Mirmiran and Shahawy (1997). The parameters in this model are obtained by a statistical analysis of the experimental results available in the literature. The final expression is based on the properties of FRP and concrete, regardless of the type of FRP used, and it is given by the following expression:

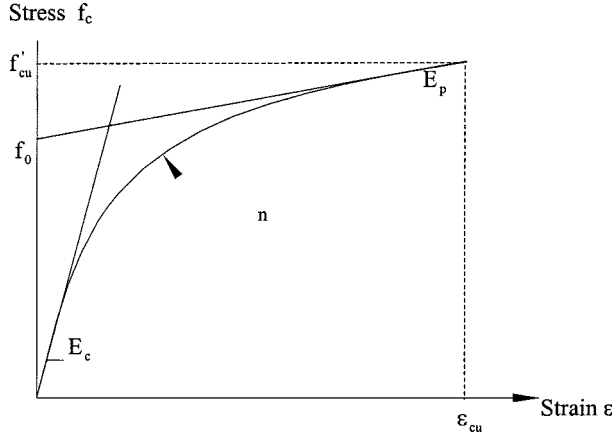


Fig. 1 Proposed stress-strain model for FRP wrapped concrete

$$f_c = \frac{(E_c - E_p)\varepsilon}{\left[1 + \left(\frac{(E_c - E_p)\varepsilon}{f_0}\right)^n\right]^{1/n}} + E_p\varepsilon \quad (1)$$

where the basic parameters are shown in Fig. 1 and are defined as

E_c = initial tangent modulus of unconfined normal weight concrete, which according to the ACI code is given by:

$$E_c = 57.0\sqrt{1000f'_c} \quad (\text{ksi}) \quad (2)$$

where f'_c (ksi) is the compressive strength of unconfined concrete.

E_p = second slope (plastic slope) of the stress-strain curve. It is given by

$$E_p = -113.3 + 42.4 \times f'_c + 0.66 \frac{E_j t_j}{D_c} \quad (\text{ksi}) \quad (3)$$

where E_j (ksi), t_j (in) are the elastic modulus and thickness of FRP wrap, respectively, and D_c (in) is the diameter of the concrete specimen.

f_0 = plastic stress at the intercept of the plastic slope with the stress axis. It is given by

$$f_0 = -1.31 + 1.15 \times f'_c + 0.02 \frac{E_j t_j}{D_c} \quad (\text{ksi}) \quad (4)$$

n = curve-shaped parameter

The initial tangent modulus of unconfined concrete, E_c , has been found to have almost the same value as that of confined concrete. Therefore, Eq. (2) given in the ACI code is used. As it can be seen in this equation, E_c is a function of only the compressive strength of unconfined concrete, f'_c (ksi). This is because the confinement is not fully activated until the concrete core reaches a large lateral expansion, i.e., an axial strain corresponding to the vicinity of the peak strength of unconfined concrete. As the axial

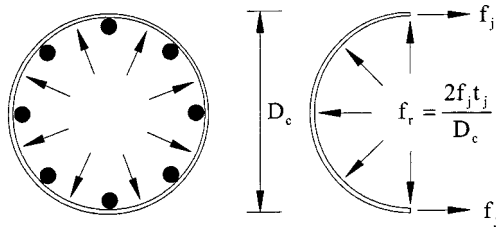


Fig. 2 Free body diagram for the calculation of the confining pressure

strain further increases, concrete cracking continues to grow and the lateral expansion of concrete increases nonlinearly. At this stage, the FRP wrap becomes the main load carrying material in the composite system. Therefore, E_p and f_0 are functions of the stiffness of FRP and the strength of unconfined concrete, and are given by Eqs. (3) and (4), respectively. The curve-shaped parameter n normally ranges from 1.0 to 2.0, and it is usually taken as $n = 1.5$ for most of cases.

Failure of FRP wrapped concrete is assumed to occur when the first ply of the FRP wraps fractures. After the first ply fracture, there is a sudden drop in the load carrying capacity of the concrete core due to a reduction in confinement. This state of failure corresponds to the ultimate strain ε_{cu} and ultimate strength f'_{cu} of confined concrete. To determine the ultimate strain ε_{cu} , the equation, $\varepsilon_{cu} = (f'_{cu} - f_0)/E_p$, is adopted, based on the geometry of the model. The ultimate strength of confined concrete f'_{cu} is given by

$$f'_{cu} = f'_c + 2.4 \times f_r \quad (\text{ksi}) \quad (5)$$

where $f_r = (2f_j t_j)/D_c$ is the confining pressure provided by the FRP wraps (Fig. 2), and f_j is the tensile strength of the FRP wraps.

It should be noted that the present model does not consider the confinement contribution of any existing steel transverse reinforcement. This is because the ultimate goal of the present research is to provide a quick way for engineers to predict the strength of a deteriorated column wrapped with FRP. In these cases, such reinforcement may be inadequate to begin with. Also, with this assumption a conservative estimate of the strength of these systems is obtained.

5. Verification of the proposed model

To verify the proposed model, a comparison with experimental results is necessary. In this section, the ultimate strength of FRP wrapped concrete (Eq. 5) and the proposed stress-strain model (Eq. 1) are verified.

Table 1 shows experimental and predicted results for the ultimate strength of FRP wrapped concrete. A description of these experiments can be found in Cheng *et al.* (2000). As it can be seen, a good prediction of the ultimate strength is achieved. This indicates that there is a linear trend in the enhancement of concrete strength as the confining pressure increases. Eq. (5) can then be used to determine the ultimate state of the proposed model.

Fig. 3 shows the predicted stress-strain curve and test results of Demers and Neale (1994) for two of their specimens. One (R44C3) had unconfined normal weight concrete strength of 6.33 ksi and it was

Table 1 Experimental vs. predicted results for ultimate strength of FRP wrapped concrete

Source	Sample no.	f'_c (ksi)	D_c (in)	f_j (ksi)	t_j (in)	f_r (a) (ksi)	$(f'_{cu})_{exp.}$ (ksi)	$(f'_{cu})_{pred.}$ (b) (ksi)	$\frac{(f'_{cu})_{exp.}}{(f'_{cu})_{pred.}}$
Demers & Neale (1994)	R32C1	4.66	6	183.5	0.01181	0.722	5.954	6.394	0.93
	R32G3-A	4.66	6	91.1	0.04134	1.255	6.997	7.671	0.91
	R32G3-B	4.66	6	91.1	0.04134	1.255	6.997	7.671	0.91
	R44C1-A	6.33	6	183.5	0.01181	0.722	7.011	8.064	0.87
	R44C3-A	6.33	6	183.5	0.03543	2.167	10.893	11.531	0.94
	R44C3-B	6.33	6	183.5	0.03543	2.167	10.633	11.531	0.92
Picher et al. (1996)	C0	5.75	6	101	0.03543	1.193	8.108	8.613	0.94
	C6	5.75	6	85.4	0.03543	1.009	7.590	8.171	0.93
	C12	5.75	6	71.8	0.03543	0.847	7.878	7.784	1.01
Karbhari & Howie (1997)	O	5.56	6	115.2	0.01299	0.499	6.500	6.757	0.96
	O2	5.56	6	151.7	0.02598	1.314	8.645	8.714	0.99
	O3	5.56	6	159.8	0.03898	2.076	11.253	10.544	1.07
	O4	5.56	6	195.8	0.05197	3.392	12.962	13.700	0.95
Mirmiran et al. (1998) (1) length effect (2) bond effect	S6-12-1	6.5	6	76	0.057	1.444	9.140	9.966	0.92
	S6-12-2	6.5	6	76	0.057	1.444	8.270	9.966	0.83
	S10-12-1	6.5	6	84	0.087	2.436	12.070	12.346	0.98
	S10-12-2	6.5	6	84	0.087	2.436	10.930	12.346	0.89
	S14-12-1	6.5	6	93	0.117	3.627	15.160	15.205	1.00
	R3BA	4.52	6	85	0.0744	2.108	9.778	9.579	1.02
	R3BB	4.52	6	85	0.0744	2.108	9.369	9.579	0.98
	R5BA	4.52	6	85	0.124	3.513	13.184	12.952	1.02
	R5BB	4.52	6	85	0.124	3.513	14.032	12.952	1.08
	R3UBA	4.52	6	85	0.0744	2.108	9.139	9.579	0.95
	R3UBB	4.52	6	85	0.0744	2.108	9.478	9.579	0.99
	R5UBA	4.52	6	85	0.124	3.513	13.314	12.952	1.03
	R5UBB	4.52	6	85	0.124	3.513	12.894	12.952	1.00
Mirmiran & Shahawy (1997)	DA11	4.476	6	76	0.0568	1.439	7.782	7.929	0.98
	DA13	4.476	6	76	0.0568	1.439	8.194	7.929	1.03
	DA21	4.476	6	84	0.0868	2.430	10.567	10.309	1.03
	DA23	4.476	6	84	0.0868	2.430	11.311	10.309	1.10
	DA31	4.476	6	93	0.1168	3.621	12.432	13.166	0.94
	DA33	4.476	6	93	0.1168	3.621	12.583	13.166	0.96
	DB12	4.299	6	76	0.0568	1.439	8.019	7.752	1.03
	DB13	4.299	6	76	0.0568	1.439	8.735	7.752	1.13
	DB21	4.299	6	84	0.0868	2.430	10.813	10.132	1.07
	DB23	4.299	6	84	0.0868	2.430	10.405	10.132	1.03
	DB31	4.299	6	93	0.1168	3.621	12.505	12.989	0.96
	DB33	4.299	6	93	0.1168	3.621	12.681	12.989	0.98
	DC11	4.637	6	76	0.0568	1.439	8.566	8.090	1.06
	DC12	4.637	6	76	0.0568	1.439	8.816	8.090	1.09

Table 1 (Continued)

Source	Sample no.	f'_c (ksi)	D_c (in)	f_j (ksi)	t_j (in)	f_r (a) (ksi)	$(f'_{cu})_{exp.}$ (ksi)	$(f'_{cu})_{pred.}$ (b) (ksi)	$\frac{(f'_{cu})_{exp.}}{(f'_{cu})_{pred.}}$
Mirmiran & Shahawy (1997)	DC21	4.637	6	84	0.0868	2.430	11.218	10.470	1.07
	DC22	4.637	6	84	0.0868	2.430	11.179	10.470	1.07
	DC31	4.637	6	93	0.1168	3.621	12.489	13.327	0.94
	DC32	4.637	6	93	0.1168	3.621	12.182	13.327	0.91
Harries <i>et al.</i> (1998)	E-glass-1	3.8	6	2.182	1	0.727	5.57	5.546	1.00
	E-glass-2	3.8	6	2.182	2	1.455	7.61	7.291	1.04
	Carbon-1	3.8	6	3.312	1	1.104	7.34	6.450	1.14
	Carbon-2	3.8	6	3.312	2	2.208	9.28	9.099	1.02

(a): $f_r = (2f_j t_j)/D_c$

(b): $(f'_{cu})_{pred.} = f'_c + 2.4 \times f_r$

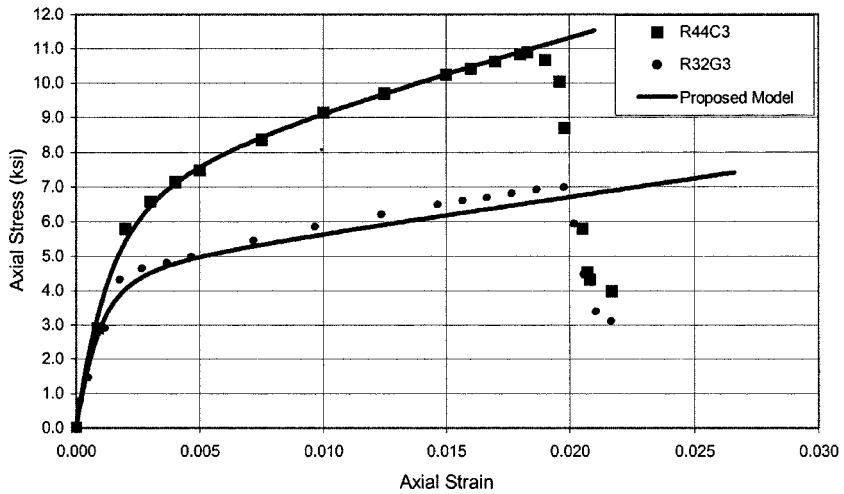


Fig. 3 Comparison of model with test results by Demers & Neale (1994)

wrapped with three layers of carbon FRP having tensile strength and elastic modulus of 183.5 ksi and 12071.5 ksi, respectively. Another (R32G3) had unconfined concrete strength of 4.66 ksi and it was wrapped with three layers of glass FRP having tensile strength and elastic modulus of 91.1 ksi and 4345.7 ksi, respectively. As it can be seen from this figure, a good agreement between results is achieved.

Fig. 4 shows the comparison of the predicted stress-strain curve and the test results by Mirmiran and Shahawy (1997) for three of their specimens. Three specimens (DA13, DB21, DC32) had unconfined concrete strength of 4.476, 4.299, 4.637 ksi, and were cast into E-glass FRP tubes which had tensile strength, elastic modulus, and the thickness of 84 ksi, 5850 ksi, 0.0868 in, 76 ksi, 5400 ksi, 0.0568 in, and 93 ksi, 5940 ksi, 0.1168 in, respectively. A good agreement is again

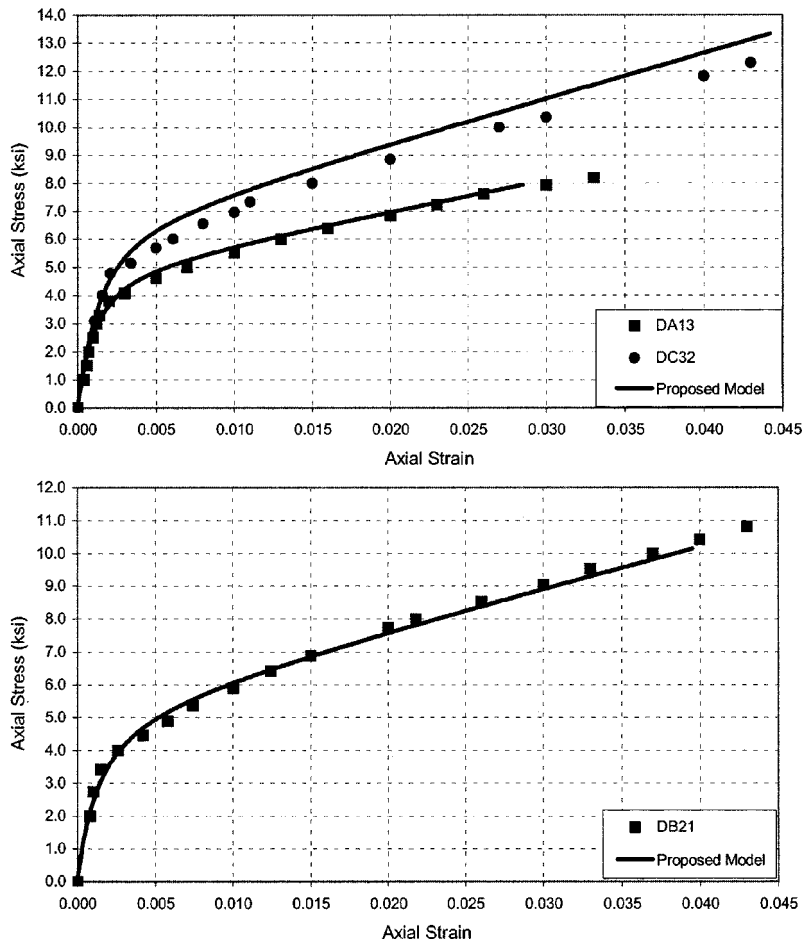


Fig. 4 Comparison of model with test results by Mirmiran & Shahawy (1997)

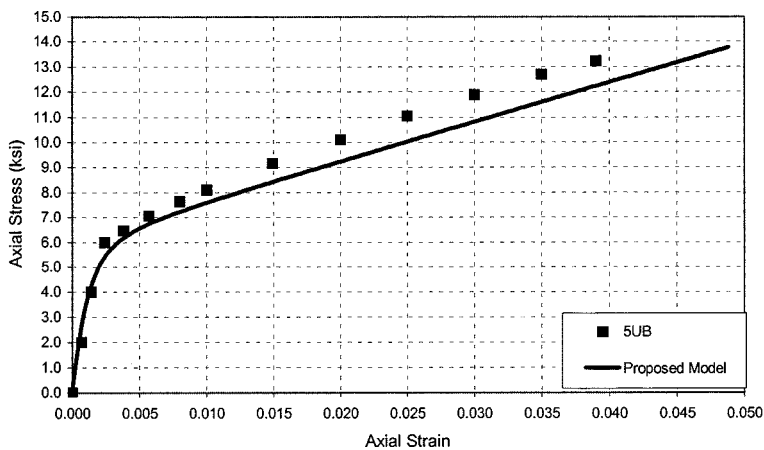


Fig. 5 Comparison of model with test results by Mastrapa (1997)

observed.

Fig. 5 shows the predicted stress-strain curve and the test results by Mastrapa (1997) for one of his FRP-wrapped specimens with five layers of S-glass FRP. The concrete strength was 5.4 ksi while the tensile strength and the elastic modulus of the FRP jackets were 85 and 2984 ksi, respectively. A good correlation is once again obtained.

6. Moment-curvature relations

6.1. Basic assumptions

This work adopts some widely used assumptions in the derivation of the moment-curvature, $M-\phi$, relations. They are:

- (1) Plane sections remain plane before and after bending.
- (2) Strain compatibility between concrete and steel in any section is assumed; the strain in the reinforcement is equal to the strain in the concrete at the same level. This implies a perfect bond between these two materials.
- (3) The tensile strength of concrete is neglected.
- (4) Concrete is assumed to fail when the compressive strain of FRP wrapped concrete reaches the maximum value. This maximum compressive strain is equal to the ultimate compressive strain ε_{cu} in the stress-strain model of FRP wrapped concrete. This is because FRP wrapped concrete does not fail until FRP materials fracture.
- (5) The developed compressive stress-strain relation for FRP wrapped concrete is adopted.
- (6) A typical idealized stress-strain curve for steel, which is assumed to behave as an elastic-perfectly plastic material, is assumed.

7. Derivation

A typical FRP wrapped reinforced concrete circular column section is shown in Fig. 6(a). It consists of three components: FRP composite, concrete, and steel. The FRP wrap serves mainly as confinement for concrete and its effects on the compressive stress and the compressive strain of concrete are accounted for in the stress-strain relation for concrete. In the present work, the equivalent section shown in Fig. 6(b), thus, does not show the FRP composite. Furthermore, a ring of the same material can replace the longitudinal reinforcement with the same area as the longitudinal reinforcement. Therefore, the equivalent column section (Fig. 6(b)) replaces the original one and is used in the following to derive the $M-\phi$ relations. This equivalent column section is further decomposed into several simple solid circular sections shown in Figs. 6(c), (d), (e), (f), and (g). This decomposition is used primarily to simplify the computations.

The basic principles of equilibrium and compatibility are used here to compute the columns strength. Consider an FRP wrapped reinforced concrete circular column section, which is subjected to an axial force P (positive in compression) at the centroid and to a bending moment M . The axial force is assumed to be applied first and maintained at a constant value, then the bending moment is continuously increased from zero to its maximum. Because of the assumption that plane sections remain plane after bending, the strain distribution is linear throughout the depth of the section. The strain in the fiber that is away from the centroid line by distance y can be expressed in terms of the mean strain ε_0 , due to axial load, and the

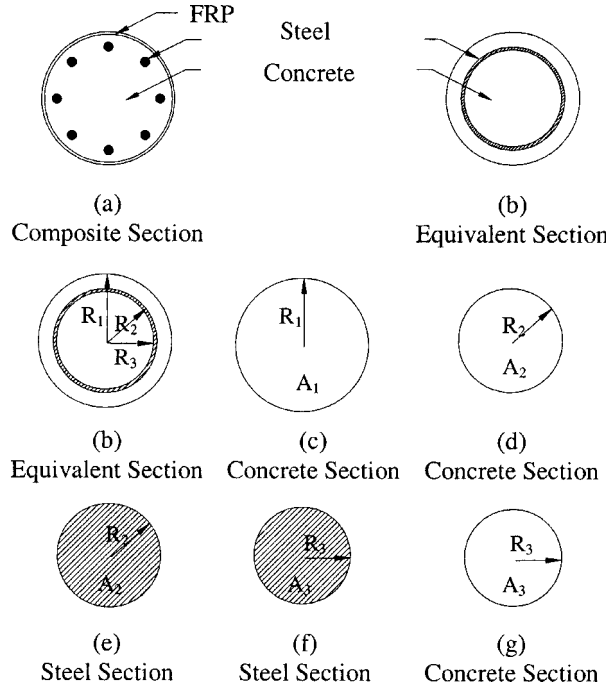


Fig. 6 FRP wrapped reinforced concrete cross section characteristics

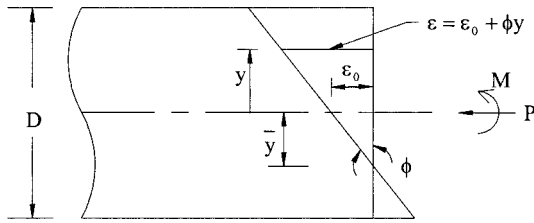


Fig. 7 Strain distribution of a section

curvature ϕ by $\epsilon = \epsilon_0 + \phi y$ (Fig. 7), and the distance of the neutral axis, \bar{y} , is obtained by $\bar{y} = \frac{-\epsilon_0}{\phi}$.

The stresses in the concrete (f_c) and in the steel (f_s) are expressed as functions of ϵ_0 , ϕ and y as

$$f_c = f_c(\epsilon) = f_c(\epsilon_0, \phi, y) \quad (6)$$

$$f_s = f_s(\epsilon) = f_s(\epsilon_0, \phi, y) \quad (7)$$

Depending on the position of the neutral axis \bar{y} and the value of the strain in the top fiber of concrete in compression, and using the principle of superposition (Figs. 6(b)~(g)), the axial force P can be expressed as shown in Fig. 8 by

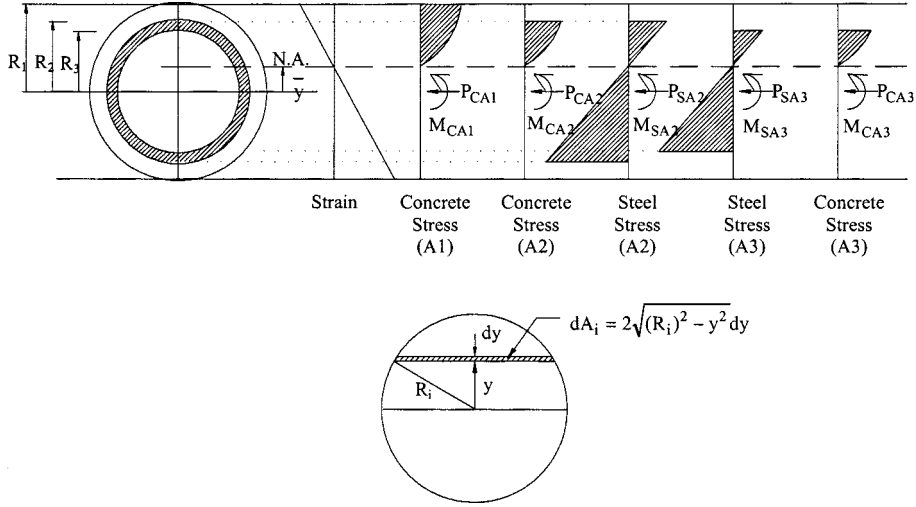


Fig. 8 Distribution of strain and stress

$$P = \int f \cdot dA = P_{CA1} - P_{CA2} + P_{SA2} - P_{SA3} + P_{CA3} \quad (8)$$

where

$$P_{CAi} = \text{compressive force in the concrete section } A_i; P_{CAi} = \int_{A_i} f_c \cdot dA_i, \quad i = 1 \sim 3$$

$$P_{SAj} = \text{net compressive force in the steel section } A_j; P_{SAj} = \int_{A_j} f_s \cdot dA_j, \quad j = 2 \sim 3$$

$$dA_i = 2\sqrt{(R_i)^2 - y^2} dy, \quad i = 1 \sim 3$$

Substituting for the stresses expressed by Eqs. (6) and (7), the axial force P is obtained as

$$\begin{aligned} P = & \int_{-R_1}^y f_c(\varepsilon_0, \phi, y)(2\sqrt{(R_1)^2 - y^2} dy) - \int_{-R_2}^y f_c(\varepsilon_0, \phi, y)(2\sqrt{(R_2)^2 - y^2} dy) \\ & + \int_{-R_2}^{R_2} f_s(\varepsilon_0, \phi, y)(2\sqrt{(R_2)^2 - y^2} dy) - \int_{-R_3}^{R_3} f_s(\varepsilon_0, \phi, y)(2\sqrt{(R_3)^2 - y^2} dy) \\ & \int_{-R_3}^y f_c(\varepsilon_0, \phi, y)(2\sqrt{(R_3)^2 - y^2} dy) \end{aligned} \quad (9a)$$

or

$$P = P(\varepsilon_0, \phi) \quad (9b)$$

Similarly, the corresponding bending moment M is given by

$$\begin{aligned} M = & \int_{-R_1}^y f_c(\varepsilon_0, \phi, y)(y)(2\sqrt{(R_1)^2 - y^2} dy) - \int_{-R_2}^y f_c(\varepsilon_0, \phi, y)(y)(2\sqrt{(R_2)^2 - y^2} dy) \\ & + \int_{-R_2}^{R_2} f_s(\varepsilon_0, \phi, y)(y)(2\sqrt{(R_2)^2 - y^2} dy) - \int_{-R_3}^{R_3} f_s(\varepsilon_0, \phi, y)(y)(2\sqrt{(R_3)^2 - y^2} dy) \\ & \int_{-R_3}^y f_c(\varepsilon_0, \phi, y)(y)(2\sqrt{(R_3)^2 - y^2} dy) \end{aligned} \quad (10a)$$

or

$$M = M(\varepsilon_0, \phi) \quad (10b)$$

Nondimensional variables are defined here as

$$m = \frac{M}{M_b}; \quad \varphi = \frac{\phi}{\phi_b}; \quad p = \frac{P}{P_0} \quad (11)$$

where M_b is the balanced moment which causes concrete to reach its maximum compressive strain and steel to reach its yield strain, simultaneously; P_b and ϕ_b are the corresponding balanced axial load and balanced curvature, respectively. P_0 is defined by $P_0 = f'_{cu} A_c + f_y A_s$, where f'_{cu} is the maximum compressive stress of FRP wrapped concrete; A_c and A_s are areas of the concrete section and longitudinal steel, respectively.

The axial force and the bending moment expressed by Eqs. (9b) and (10b) are further simplified by

$$p = p(\varepsilon_0, \varphi) \quad (12)$$

$$m = m(\varepsilon_0, \varphi) \quad (13)$$

It is found that the axial force and the bending moment are functions of the mean strain ε_0 and the curvature φ . Elimination of ε_0 from these two equations gives a relationship among the bending moment m , the curvature φ , and the axial force p . Direct elimination, however, is not possible, because of the nonlinearity in the concrete stress-strain model. A trial and error method is adopted to obtain the strain distribution so that the summation of stresses is equal to the applied force. The resulting moment and curvature corresponding to this particular axial force are then obtained. A computer program has been developed to perform the required computations. Two examples are given in the next section using the developed program.

8. Examples

8.1. Reinforced concrete section with unconfined concrete stress-strain model

The unconfined concrete stress-strain model proposed by Hognestad (1951) is used here to develop the $m-\varphi$ curves for the reinforced concrete circular column section (without FRP wraps) (Fig. 9). The

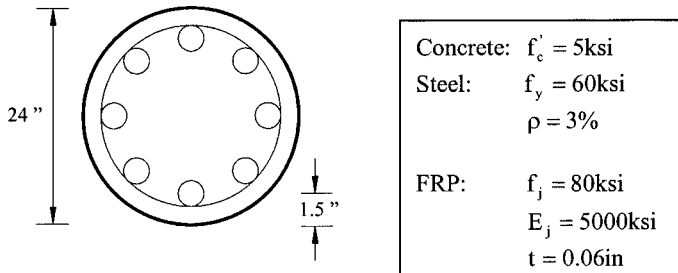


Fig. 9 Properties and geometry of RC column section

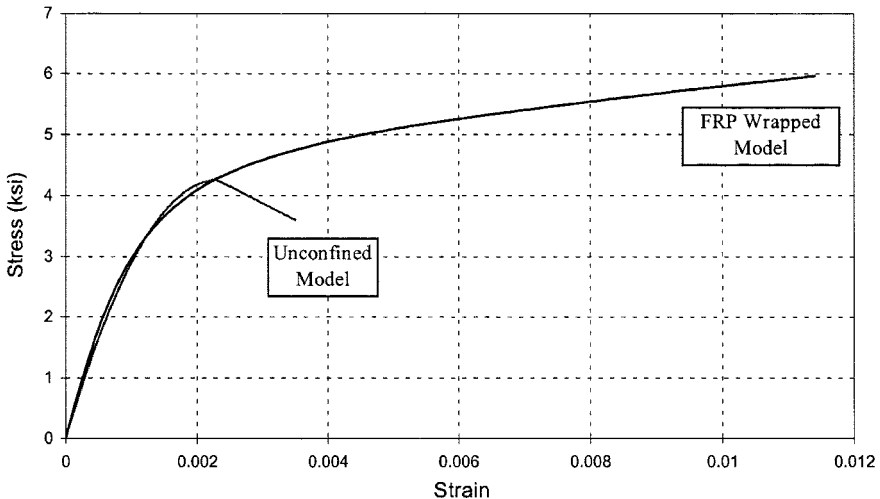


Fig. 10 Stress-strain model for unconfined concrete and FRP wrapped concrete

steel ratio is defined as the ratio of the area of longitudinal reinforcement to the gross area of the cross section. The stress-strain model is a second order parabolic curve up to the maximum stress followed by a straight line and the ultimate compressive strain is assumed to be 0.0035, which is shown in Fig. 10.

8.2. Reinforced concrete section with FRP wrapped concrete stress-strain model

The same reinforced concrete circular section (Fig. 9) wrapped with FRP composite is considered in this example. The stress-strain curve of FRP wrapped concrete is obtained based on the proposed model and is also shown in Fig. 10 for comparison. It is obvious that the confinement provided by the FRP wrap significantly increases the compressive strain of concrete as well as its compressive stress.

9. Comparison

For the reinforced concrete column section using the Hognestad's concrete model, the $m-\varphi$ curves are shown in Fig. 11. As it can be seen from this figure, the axial load has a major influence on the moment capacity and on the initial stiffness (i.e., the slopes of $m-\varphi$ curves) of the cross section. Balanced failure in which crushing of concrete and yielding of tension steel are developed simultaneously occurs in this example as the balanced moment m_b is 1.0 and the balanced load p_b is 0.358. This state of balanced failure represents the change from tension-controlled failure for lower loads to compression-controlled failure for higher loads. In the state of tension-controlled failure (Fig. 11a), zero axial load gives the minimum moment capacity and initial stiffness of the cross section. As the axial load increases up to the balanced load p_b , the moment capacity increases as well. However, as the axial load increases beyond the balanced load, the moment capacity decreases. This state of failure is referred to as compression-controlled failure and is shown in Fig. 11b.

It should be noted that the balanced moment m_b is not always the maximum moment capacity of the

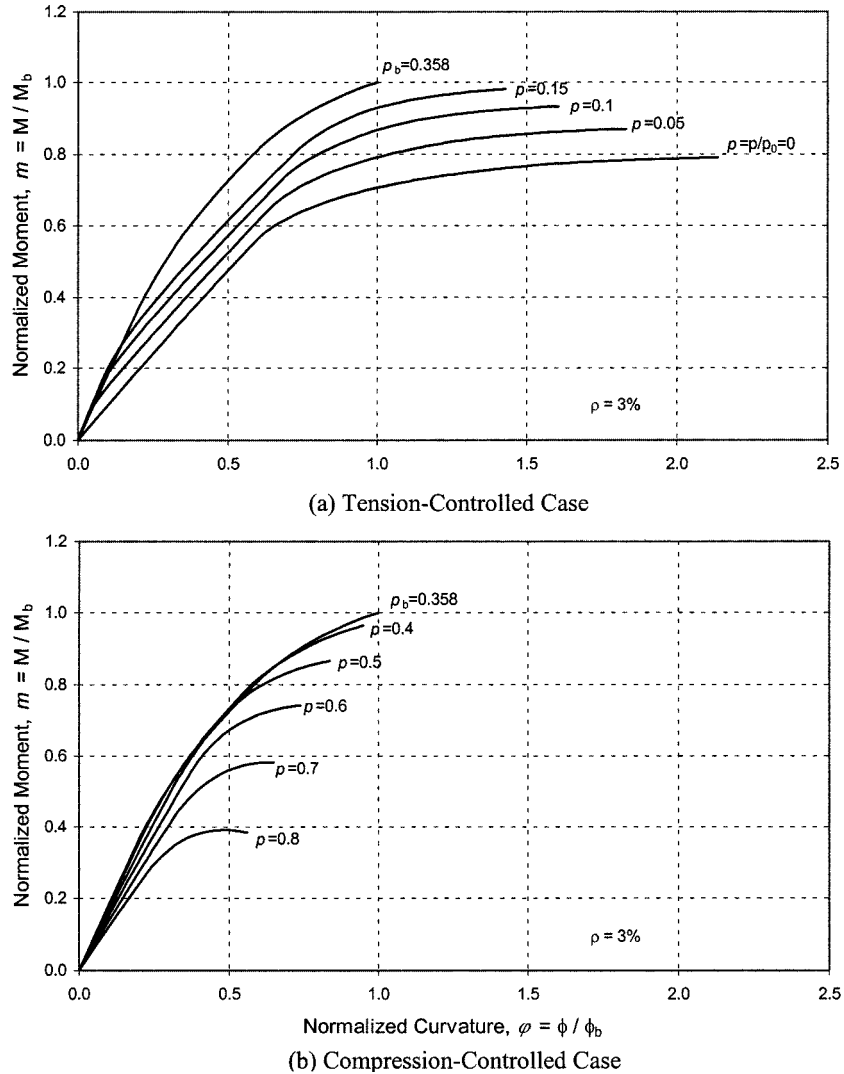


Fig. 11 Moment-curvature relationships for unconfined concrete model (3%). ($M_b = 8824.4$ k-in, $P_b = 959.6$ kip, $\phi_b = 0.00025$)

cross section, although the state of balanced failure is a point of bifurcation between tension-controlled failure and compression-controlled failure (Fig. 11). In this example, the maximum moment capacity of the cross section occurs under the normalized load of 0.3. However, the difference of the balanced moment to the maximum moment is small (3%). This can be seen in the interaction diagram of the cross section (Fig. 12).

The effect of the axial load on the initial stiffness can also be observed in Fig. 11. It is found that the initial stiffness in the compression-controlled case does not vary as much as in the tension-controlled case, although the variation is still significant. The variations of the initial stiffness in both cases, however, are minimized as the steel ratio ρ increases (Chen and Chen 1974).

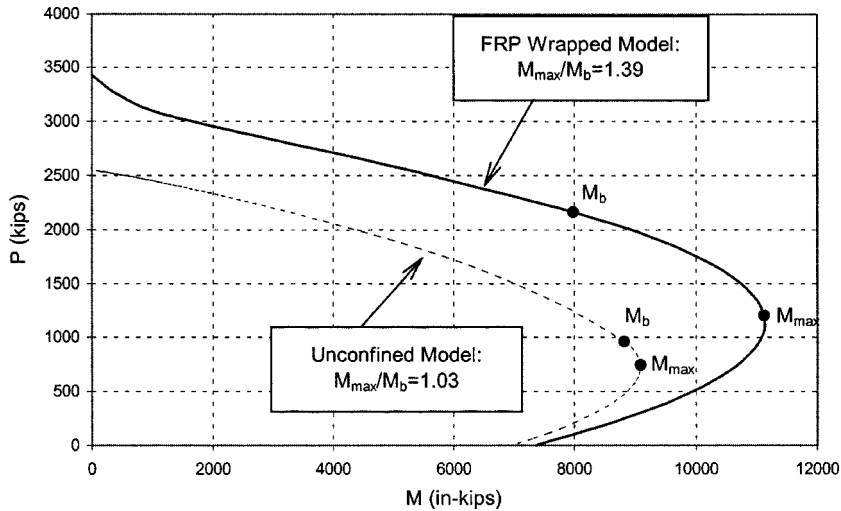


Fig. 12 Interaction diagram

For the reinforced concrete column section with the FRP wrapped concrete model, the $m-\varphi$ curves shown in Fig. 13 show that the axial load also has a major influence on the moment capacity and on the initial stiffness as the previous example. Balanced failure occurs under the balanced moment m_b of 1.0 and the balanced load p_b of 0.63 in this example. In the state of tension-controlled failure (Fig. 13a), as the axial load increases up to the balanced load p_b , the moment capacity increases first and then decreases. This implies that the maximum moment capacity of the cross section occurs in a tension-controlled state. The difference between the balanced moment and the maximum moment is 39% in this case. This is significantly different from the previous example, and it can be attributed mainly to the change in the concrete stress-strain model. This difference is also depicted in Fig. 12. Besides, the increase in the loading capacity due to the confinement provided by FRP wraps is also observed in this figure. In the state of compression-controlled failure, as the axial load increases beyond the balanced load, the moment capacity decreases. This is the same phenomenon as the previous example and is shown in Fig. 13b.

The effect of the axial load on the initial stiffness can be seen again in Fig. 13. No consistent trends can be detected. However, the variations of the initial stiffness in both cases are minimized as the steel ratio r increases (Cheng *et al.* 2000).

10. Conclusions

The present work is concerned with the use of FRP for corrosion protection reinforced concrete columns, which is very important in cold-weather and coastal regions. More specifically, it is intended to give practicing engineers with a more practical procedure for estimating the strength of a deficient column rehabilitated using FRP wrapped columns than those currently available. To achieve this, a stress-strain model for FRP wrapped concrete has been developed and verified using experimental results from different studies and good correlation has been observed. An analysis is also carried out to

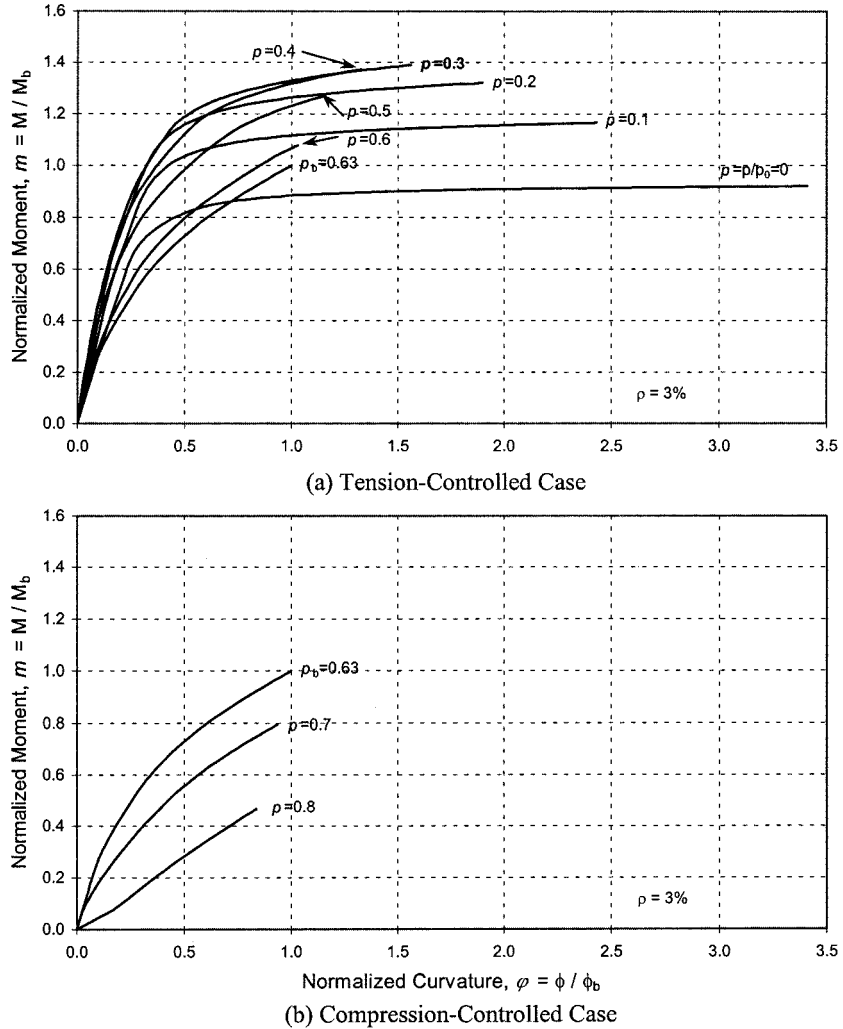


Fig. 13 Moment-curvature relationships for FRP-confined concrete model ($\rho = 3\%$). ($M_b = 7987.5$ k-in, $P_b = 2160.1$ kip, $\phi_b = 0.00062$)

develop the moment-curvature relations for an FRP wrapped reinforced concrete circular column section. This analysis uses the developed stress-strain model of FRP wrapped concrete and a typical idealized stress-strain curve for the steel. It is found that due to the confinement provided by the FRP wraps, the concrete stress-strain model changes significantly. This in turn causes the move of the maximum moment of the cross section from a position close to the balanced moment to a position away from the balanced moment in the moment-curvature curves and the interaction diagram. This suggests that the balanced moment m_b is no longer a critical moment in the interaction curve. The obtained moment-curvature curves and the interaction diagram are being used in the development of a design equation, which is intended to help engineers to take advantage of these systems in civil infrastructure with more confidence.

References

- Chen, W.F. and Chen, A.C.T. (1974), "Strength of laterally loaded reinforced concrete columns", *IABSE Symposium on Design and Safety of Reinforced Concrete Compression Members, Quebec, Preliminary Publication*, 315-322.
- Cheng, H.L., Sotelino, E.D. and Chen, W.F. (2000), "Moment-curvature relations for FRP wrapped reinforced concrete columns", Department Report, CE-STR-00-2, School of Civil Engineering, Purdue University, West Lafayette, IN.
- Demers, M. and Neale, K.W. (1994), "Strengthening of concrete columns with unidirectional composite sheets", *Developments in Short and Medium Span Bridge Engineering 94*, ACM in Structures, 895-905.
- Fardis, M.N. and Khalili, H. H. (1981), "Concrete encased in fiberglass-reinforced plastic", *ACI J.*, **78**(6), 440-446.
- Fardis, M.N. and Khalili, H.H. (1982), "FRP-encased concrete as a structural material", *Mag of Concrete Res.*, **34**(121), 191-202.
- Howie, I. and Karbhari, V.M. (1995), "Effect of tow sheet composite wrap architecture on strengthening of concrete due to confinement: I-experimental studies", *J. Reinforced Plastics and Composites*, **14**, 1008-1030.
- Karbhari, V.M. and Howie, I. (1997), "Effect of composite wrap architecture on strengthening of concrete due to confinement: II-strain and damage effects", *J. Reinforced Plastics and Composites*, **16**(11), 1039-1063.
- Lan, Y.M., Sotelino, E.D. and Chen, W.F. (1998), "State-of-the-art review of highway bridge columns retrofitted with FRP jackets", Department Report, CE-STR-98-5, School of Civil Engineering, Purdue University, West Lafayette, IN.
- Mastrapa, J.C. (1997), "Effect of bonded and unbonded construction on confinement with fiber composite", M.S. thesis, University of Central Florida, Orlando, FL.
- Mirmiran, A. and Shahawy, M. (1997), "Analytical and experimental investigation of reinforced concrete columns encased in fiberglass tubular jacket and use of fiber jacket for pile splicing", Final Report, The Florida Department of Transportation, February.
- Nanni, A. and Bradford, N.M. (1995), "FRP jacketed concrete under uniaxial compression", *Constr. & Bldg. Mat.*, **9**(2), 115-124.
- Picher, F., Rochette, P. and Labossiere, P. (1996), "Confinement of concrete cylinders with CFRP", *Proc. of the First International Conference on Composites in Infrastructure*, ICCI96, 829-841.
- Priestley, M. J. N. and Seible, F. (1991), "Seismic assessment and retrofit of bridges", *Struct. Sys. Res. Proj. Report No. SSRP-91/03*, University of California at San Diego, Calif.
- Priestley, M.J.N., Seible, F. and Calvi, G.M. (1996), *Seismic Design and Retrofit of Bridges*, John Wiley & Sons, Inc., New York, NY.
- Saadatmanesh, H., Ehsani, M.R. and Li, M.W. (1994), "Strength and ductility of concrete columns externally reinforced with fiber composite straps", *ACI Struct. J.*, **91**(4), 434-447.
- Saadatmanesh, H., Ehsani, M.R. and Jin, L. (1996) "Seismic strengthening of circular bridge pier models with fiber composites", *ACI Struct. J.*, **93**(6), 639-647.
- Saenz, L. P. (1964), "Equation of the stress-strain curve of concrete", Discussion of the Paper, *ACI J., Proceedings* **61**(9), 1227-1239.
- Seible, F., Davol, A. Burgueno, R. Nuismier, R.J. Abdallah, M.G. (1996), "Structural behavior of concrete filled carbon fiber composite tubular columns", *Proceedings of the 1996 28th International SAMPE Technical Conference*, Seattle, WA, USA. November 04-07, 1258-1269.
- Seible, F. and Priestley, M.J.N. (1993), "Retrofit of rectangular flexural columns with composite fiber jackets", *Proceedings of 2nd Annual Seismic Research Workshop*.
- Seible, F., Priestley, M.J.N., Hegemier, G.A. and Innamorato, D. (1997), "Seismic retrofit of RC columns with continuous carbon fiber jackets", *J. Compos. Constr.*, **1**(2), 52-62.
- Spoelstra, M.R. and Monti, G. (1999), "FRP-confined concrete model", *J. Compos. Constr.*, **3**(3), 143-150.
- Teng, M.H., Sotelino, E.D. and Chen, W.F. (2000). "Monitoring of long-term performance of highway bridge columns retrofitted by advanced composite jackets in Indiana," INDOT Draft Report, SPR-2161.
- Xiao, Y. and Ma, R. (1997), "Seismic retrofit of RC circular columns using prefabricated composite jacketing", *J. Struct. Engrg., ASCE*, **123**(10), 1357-1364.
- Xiao, Y., Martin, G.R., Yin, Z. and Ma R. (1996), "Seismic retrofit of existing reinforcement concrete bridge

- columns using a prefabricated composite jacking system”, *Proc. of the First International Conference on Composites in Infrastructure*, ICCI96, 903-916.
- Xiao, Y. and Wu, H. (2000), “Compressive behavior of concrete confined by carbon fiber composite jackets”, *J. Materials in Civil Engineering*, 12(2), 139-146.
- CU